# Conventional vs. reinforced resin injected connectors' behaviour in static, fatigue and creep experiments on slip-resistant steel-FRP joints

Olivier, Gerhard; Csillag, Fruzsina; Tromp, Elisabeth; Pavlovic, Marko

**DOI**
10.1016/j.engstruct.2021.112089

**Publication date**
2021

**Document Version**
Final published version

**Published in**
Engineering Structures

Engineering Structures 236 (2021) 112089

Contents lists available at ScienceDirect

Engineering Structures

journal homepage: www.elsevier.com/locate/engstruct

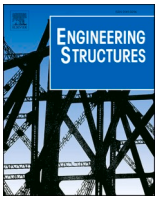

# Conventional vs. reinforced resin injected connectors' behaviour in static, fatigue and creep experiments on slip-resistant steel-FRP joints

Gerhard Olivier [a], Fruzsina Csillag [b], Elisabeth Tromp [c], Marko Pavlović [a,*]

[a] TU Delft Faculty of Civil Engineering and Geosciences, 2628 CN Delft, the Netherlands
[b] Arup Infrastructure, 1043 CA Amsterdam, the Netherlands
[c] Royal HaskoningDHV Infrastructure, 3068 AX Rotterdam, the Netherlands

ARTICLE INFO

*Keywords:*
Bolted connections
Steel-FRP bridges
Slip-resistant connections
Experiments
Fatigue
Creep
Injected bolts
Steel-reinforced resin

ABSTRACT

Due to constantly increasing traffic loads and ageing infrastructure, innovative materials for implementation in renovation and new bridge construction projects are gaining attention. One such innovation is hybrid structures consisting of Glass Fibre-Reinforced Polymer (GFRP) composite decks connected to a steel girder(s) superstructure. By combining the stiffness provided by steel members with the superior fatigue endurance and strength to weight ratio of FRP, the properties of both materials can be efficiently exploited. The main restriction to the implementation of hybrid steel-FRP structures lies in the lack of knowledge and efficient technical solutions for the connection between the two materials. Adhesively bonded and grouted connections have been identified as possible connection systems, whereas limited research has been performed on bolted connections. To address this research gap, this paper discusses an experimental investigation into the performance of two types of slip-resistant bolted connectors, namely conventional resin injected bolts and a novel connector system developed at TU Delft comprising of a bolted connector injected with steel reinforced resin (iSRR). Connectors' performance is evaluated by means of long-term (sustained and cyclic) and short-term experiments with shear load. A single-lap shear joint configuration is used to compare performance of the two connector types. A vacuum infused GFRP multi-directional laminated plate, 20 mm thick, is connected to steel plates by means of M20 bolts. Results indicate comparable stiffness, resistance and ductility of the two connector types in short-term experiments. Superior fatigue performance of iSRR connector is found with 100 times more fully reversed load cycles that are needed to reach the same failure criterion as the conventional injected bolts.

## 1. Introduction

Hybrid steel-FRP structures represent an excellent option for the renovation of bridges, where the original deck structure (steel, concrete or timber) is deteriorated, whilst the main steel load carrying members have a reduced capacity but are reasonably well-preserved. Due to its high strength-to-weight ratio, the application of FRP decks impose minimum additional weight on the existing structure. Low weight also enables prefabrication and installation of large deck segments, leading to minimum traffic hindrance which is of huge benefit in bridge infrastructure renovation projects. The success of designing competitive hybrid steel-FRP repair, as well as new built structures, heavily depends on the structural performance of the deck-to-girder connection. To visualise this scenario, Fig. 1a depicts an FRP deck placed upon a steel main load carrying structure of a bascule type movable bridge. In the case that hybrid interaction between the FRP deck and the girder is to be engaged, a slip-resistant connection is required to obtain reliable shear interaction and sufficient fatigue endurance during a bridge lifetime. Fig. 1b show a possible connection detail of the FRP deck panel to main or cross girders of a steel bridge superstructure.

Extensive research has been performed on adhesive and grouted shear stud connection between steel beams and the FRP decks, such as [1,2]. Bolted connections were rarely investigated due to the localised load transfer and/or slip behaviour, such as in case of blind-bolted connectors. Injected bolts, such as shown in Fig. 1c, can both reduce stress concentrations and offer slip-resistance. However, installation is cumbersome requiring access from both the top and bottom and need for relatively large hole, approx. 30–40 mm, in the top facing of the FRP panel which will lead to a connection detail fragile against water intrusion.

* Corresponding author.
*E-mail address:* M.Pavlovic@tudelft.nl (M. Pavlović).

https://doi.org/10.1016/j.engstruct.2021.112089
Received 15 June 2020; Received in revised form 2 February 2021; Accepted 17 February 2021
Available online 13 March 2021

Although large databases have been generated in past to characterise fatigue behaviour of GFRP laminates as material [3,4], much less data is available on fatigue of bearing type failure of the connectors. Existing research results related to fatigue testing of bolted joints between FRP and steel is mainly limited to behaviour in pultruded profiles of small thicknesses. Also, very limited information is available on fatigue behaviour of slip-resistant connectors in FRP.

Ordinary (non-preloaded and non-injected) and blind bolt connections were tested by [5] in pultruded 5.5 mm thick, GFRP (polyester resin, E-glass) in double-lap joints (DLJ). Three stress levels were applied (at 30%, 50% and 80% of static resistance of the joint) at the stress ratio of R = 0.1. Shear-out failure mode was observed for all specimens with both ordinary and blind-bolted joints in both static and fatigue loading. It was found that the static strength of the joint with blind-bolts is 21% less than ordinary bolts, while the fatigue performance is less affected, see Fig. 2a. Note that neither connector types are slip-resistant.

Van Wingerde et al. [6] examined fatigue resistance of a bolted DLJ connecting the webs of pultruded I profiles (Fiberline A/S Denmark). The performance of injected bolts (slip-resistant connectors) was compared to that of ordinary bolts with bolt hole clearance of 0.9 mm. Bearing in FRP plate was the dominant failure mode of all specimens. It was found that there is negligible difference in fatigue life between the two joint types at a load ratio of R = 0.1. However, the fatigue behaviour of injected bolted joints was significantly improved compared to ordinary bolted joints with hole clearance (by a factor of 100) under the load ratio of R = −1. The authors reported k = −5.5 and k = −9.0 as the exponent (slope) of S-N curves for ordinary bolted connection and injected bolted connection, respectively. The k exponent shows how sensitive the connection is relative to the applied stress range. The higher the k exponent is the smaller the difference is between the number of cycles to failure at different stress ranges, see Fig. 2b. A rapid increase in displacement (i.e. change of slope in the displacement vs cycles curve) was used as fatigue life criterion.

Smith et al. [7] investigated possibilities to define different failure criteria for double-lap bolted joints in (0/90) CFRP laminates under tension–tension (R = 0.1) fatigue loading. Defining a certain hole elongation (e.g. 4% of the diameter *d* is defined by ASTM [8] for static bearing resistance) value did not prove to be a reliable parameter, as it was very sensitive to bolt and washer sizes as well as hole conditions (considerable differences in hole elongation were observed within results of nominal identical specimens). Permanent joint deformation was also not found to be an appropriate failure criterion, since elastic and plastic deformation could not be easily distinguished. The authors suggest a stiffness-based failure criterion as the most reliable failure criteria for bearing damage: they identify the point at which stiffness of the joint abruptly changes. The fatigue life determined in this fashion corresponds to approximately 75% of the total fatigue life. The hole elongation that corresponds to such defined criterion is found up to 5% or 50% of bearing stiffness degradation.

Zaffari et al [9] used the limitation of joint 'slip' displacement to 0.3 mm, given in Annex G of EN1090-2:2008 [10] for slip-resistant connectors in steel structures, to establish the failure criteria for injected bolted joints in pultruded laminates. It is found that 0.3 mm limitation might be too low for connections in FRP due to visco-elastic properties of the polymeric materials. For the joint details studied in [9], it was estimated from the test results that 0.75 mm could be the maximum slip displacement after 100 years under a constant service (creep) load.

New type of injection material, steel-reinforced resin (SRR), is being developed at TU Delft. SRR is composed of a skeleton of steel particles (steel spheres of a few mm diameter) and a polymer resin. The innovation of the SRR material was pioneered by Nijgh [11] in the field of bolted connections in steel structures. According to an initial study by [11], steel reinforcement offers 1.5–2 times increased stiffness and reduces creep by roughly 40% compared to pure polymer resin.

The novel injected SRR connection (iSRR) is being developed at TU Delft. Injected SRR connector utilises improved properties of SRR injection material to create a resilient connection for FRP deck panels in hybrid steel-FRP bridges. The goal is to provide slip resistant and fatigue enduring connections for FRP components through combination of bolt preloading and injection. The main idea is to provide load transfer through a large hole in the FRP plate which improves known poor resistance of FRP to bearing stresses and to fill the space between the large hole in the FRP and the bolt with a fit-for-purpose injection material. The iSRR connector design, as shown in Fig. 1c, comprises of a rod, or bolts with coupler, clamped to a steel beam and embedded in a relatively large cylindrical hole in an FRP deck by the SRR injection piece. The installation of the iSRR connection in the deck can be done as prefabricated or at the construction site where all the work is done from

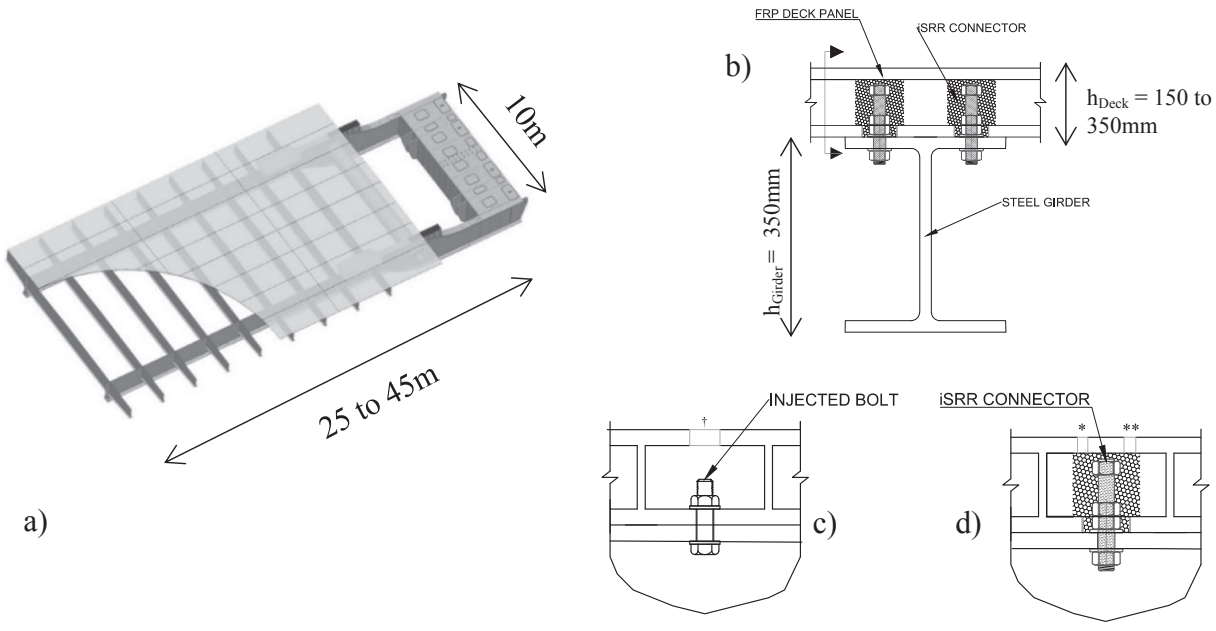


**Fig. 1.** (a) Example of FRP Deck on a movable bridge; (b) illustration of bolted connection between FRP deck panel and steel girder of the bridge; (c) details of conventional injected bolt connection († installation hole); (d) details of iSRR connector (*air release hole, **resin injection hole).

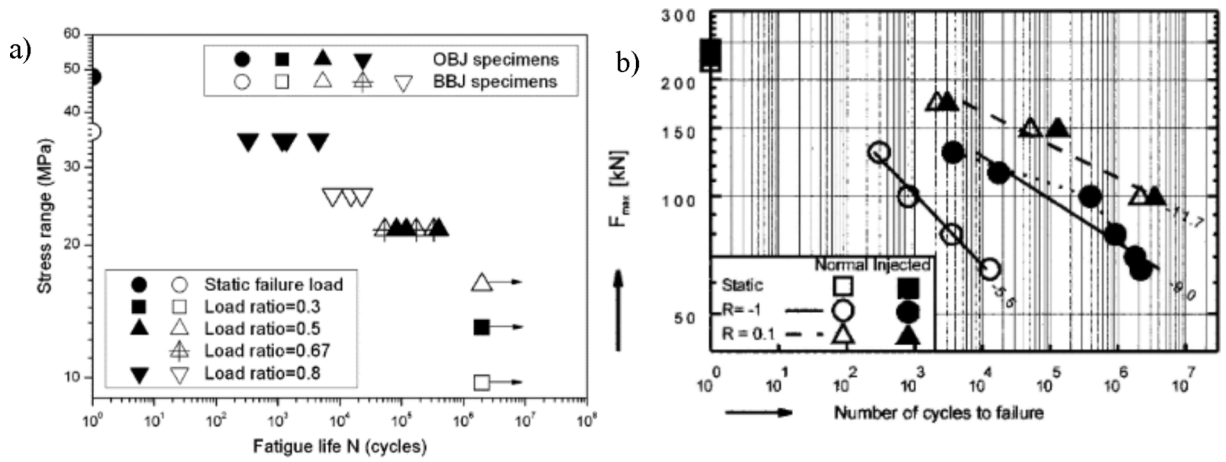


**Fig. 2.** Logarithmic S – N data of pultruded GFRP DLS joint failed by (a) shear-out failure at R = 0.1 [5] (b) failed by pin-bearing [6].

the top. In either case, after the installation of the mechanical connectors, the hole in FRP panel is filled with steel shot particles (spheres of 0.5–2.0 mm in diameter) and injected with polymer resin. A relatively large hole is drilled in the bottom facing of FRP deck, thus providing larger tolerances for execution. In case of M20 bolts, as tested here, the hole in FRP is 60 mm diameter. Once the resin is cured, slip-resistant connection is achieved by steel-reinforced resin filling the space between the mechanical connector and the hole in FRP deck. Such a connection provides demountability, large tolerances for execution as well as reduction of bearing stresses in FRP plate. Two small holes (approx. 10 mm) in the top facing are needed for installation, in contrast to large holes needed for conventional injected connectors. The design of the SRR joint offers the possibility to apply bolt preloading between the two nuts, enclosing only the steel plate in the clamping package. Exclusion of FRP plate in the clamping package solves the well-known problem of loss of bolt preloading due to poor through thickness creep performance of FRP plates. Preloading of the bolt in combination with gapless connection to FRP plate ensures long term slip-resistance. The fatigue performance of the bolted connection design is optimised by preloading the bolt, preventing slip and minimising stress concentrations in FRP plate. However, the fatigue performance of the large (~1 dl for M20 bolt) SRR injection piece, which is vital in successful load transfer mechanism, is unknown.

This paper focuses primarily on characterising fatigue and creep performance of two different types of injected slip-resistant connectors, namely conventional injected bolts (IB) and iSRR connectors. Comparable steel-FRP joint specimens of both connector types are subjected to series of static, fatigue and creep single-lap shear experiments. As the goal is to compare the performance of the connectors, the creep and fatigue experiments are of limited extent. More research is needed to define S-N and creep curves for design at different load levels.

## 2. Experimental program

To characterise the combined long- and short-term performance of the two investigated slip-resistant connector types, a set of loading regimes was applied per experimental series as shown in Table 1. Concurrently to the experimental campaign on iSRR and IB slip-resistant bolted connections, Lindapter blind-bolted connectors were also investigated although not shown in Table 1. This connector type was found to be prone to slip under cyclic loading. Results of blind-bolted connectors are discussed and compared to slip-resistant connectors in a separate paper [12].

Three loading regimes were applied to the two specimens types, namely monotonic static tensile shear loading, sustained loading and cyclic loading. Series S-iSRR and S-IB refer to iSRR and IB specimens

**Table 1**
Number of specimens per connector type and loading regimes.

| Experimental series | Sustained (creep) loading | Cyclic (fatigue) loading | Static loading |
|---|---|---|---|
| S-iSRR | | | 4 |
| S-IB | | | 3 |
| F-iSRR | | 3 | 3* |
| F-IB | | 4 | 4* |
| C-iSRR | 3 | 3+ | 3** |
| C-IB | 3 | 3+ | 3** |

* After cyclic loading.
** After sustained and cyclic loading.
\+ After sustained loading.

respectively, that were tested with static load only. Series F-iSRR, F-IB and C-iSRR, C-IB refer to specimens that were subjected first to long-term loading regime and afterwards tested for residual shear resistance in static experiments.

The naming convention is: F = cyclic (fatigue) loading; C = sustained (creep) loading + fatigue (cyclic) loading. Sustained (creep) loading of 40 kN in shear was applied for 2 months. Cyclic (fatigue) experiments were performed at fully reversed constant amplitude shear load of ±40 kN. A minimum of 3 specimens were tested per connector type and loading regime, as indicated in Table 1. In the results described in the following sections, individual specimens within an experimental series are indicated by a specimen number (i.e. C-iSRR-1 is specimen 1 of series C-iSRR). Individual specimens, in turn, consist of two connectors labelled top (T) and bottom (B) owing to specimens' vertical orientation during testing. For some analysed behaviour this enabled doubling of the number of individual results for a single test, such as: initial stiffness, slip load for iSRR, creep deformation, degradation rate during load cycles of iSRR connectors and number of cycles for IB connectors.

### 2.1. Specimens

As seen in Fig. 1c, the connectors in a real bridge deck application are located inside the FRP deck panel. In this experimental investigation, specimens were prepared in single-lap shear joint (SLJ) configurations as depicted in Fig. 3, resembling the connection of the steel plate and the bottom facing of the web-core FRP deck panel built from multi-directional laminates. As such, the webs and top facing of the FRP deck are excluded in the performed experiments. Such a set-up facilitates the observation of connection failure mechanisms, whilst providing a conservative estimate of mechanical performance for design and comparison purposes, as a higher influence of bending due to eccentricity is introduced [13]. In all specimens, a single FRP plate (160

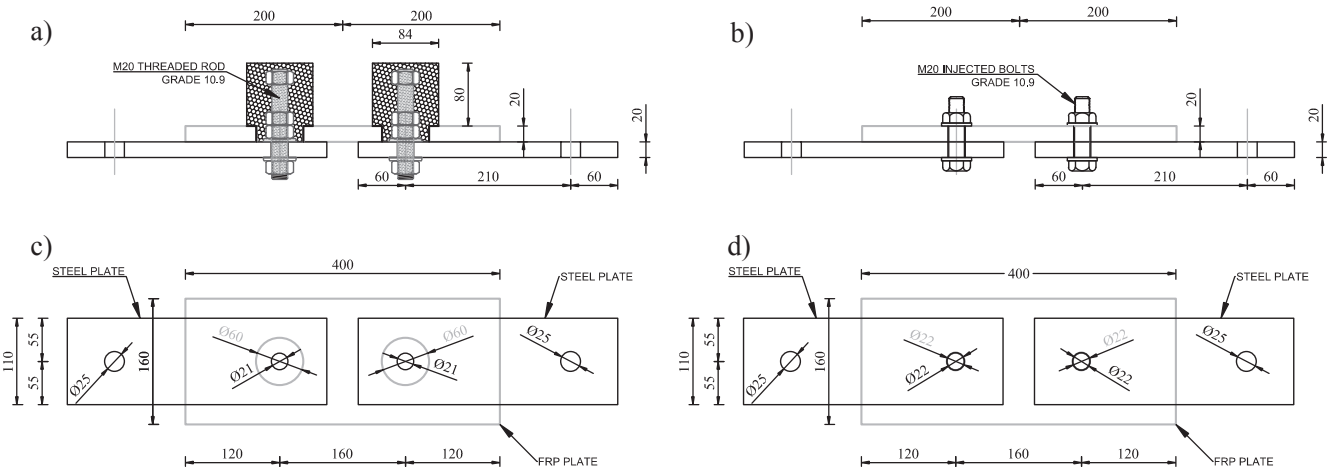


**Fig. 3.** FRP-Steel SLJ connection specimens. (a) iSRR specimen, (b) IB specimen, (c) top view iSRR specimen and (d) top view IB specimen.

mm × 400 mm × 20 mm, w × l × t) is connected to two S355 steel plates (110 mm × 330 mm × 20 mm) by means of two slip-resistant connectors as shown in Fig. 3 for both connector types.

The iSRR connectors consist of M20 threaded rods, grade 10.9, fixed to the steel plates by means of washers and nuts and subsequently pre-loaded with 550 N.m of torque. The M20 IB connectors, grade 10.9, were fabricated and installed according to the specification of EN1090-2 (Annex J) [10]. Additional geometrical details are listed in Table 2.

The vacuum-infused GFRP plates were fabricated with unidirectional and non-woven bi-directional fabrics of E-glass fibres (600–1200 g/m$^2$) and a dicyclopentadiene (DCPD) polyester resin. The stacking sequence is as follows: [90/0;$0_3$; ±$45_2$; 0/90; $0_2$; ±45; 0/90; 0]$_s$. Lay-up and stacking sequence of the laminate results in a composition of: 0°/62.5%; 90°/12.5%; +45°/12.5%; −45°/12.5%. This lay-up was selected to adhere to the requirement of at least 12.5% of fibres in each of the main material directions (0°, 90°, +45°, −45°) as specified in the design recommendation CUR96 [14]. The design fibre volume fraction is 54%. In the intended application in hybrid steel-FRP bridge structures, the orthotropic FRP deck panel is assumed to span between the main or cross girders. This means that the main interface shear forces acting on the connectors due to hybrid interaction between the FRP deck and steel girders will be perpendicular to the principal direction of fibres in the laminated plates of the FRP deck panel. Subsequently, all tested FRP specimens were orientated with their principal fibre direction perpendicular to the direction of loading. Properties of the multi-directional laminate in the direction of loading are determined according to relevant ISO and ASTM standards with at least 5 specimens with acceptable failure mode per test series. The obtained average values and variation are presented in Table 3.

The mechanical properties of the iSRR material have been tested on 150 mm long cylinders of 50 mm diameter. The average values of compression strength, Young's modulus and tension split strength are $f_c$ = 74.3 MPa, E = 9.3 GPa and $f_t$ = 10.1 MPa, respectively.

As commonly applied in practice [11], the IB connector specimens are injected with an epoxy resin (Araldite SW404 with HY2404 hardener). IB specimens were fabricated without ensuring bolts are centrally positioned within the 2 mm oversized holes (as done by [6]), to replicate the level of accuracy which is achievable in an actual full-scale installation.

**Table 2**
Specimen details.

| Specimen series | Hole diameter in steel plates | Hole diameter in FRP plate |
|---|---|---|
| S-iSRR; C-iSRR; F-iSRR | 21 mm | 60 mm |
| S-IB; C-IB; FIB | 22 mm | 22 mm |

**Table 3**
Mechanical properties of the FRP laminate in transverse direction (direction of loading).

| Mechanical Property | Average value and (CoV) |
|---|---|
| Transverse compressive strength – $f_{y,c}$ | 172 MPa (5.3%) |
| Transverse compressive modulus – $E_{y,c}$ | 19.1 GPa (6.6%) |
| Transverse tensile strength – $f_{y,t}$ | 173.7 MPa (5.2%) |
| Transverse tensile modulus – $E_{y,t}$ | 7.7 GPa (2.9%) |
| Transverse bearing strength – $f_{y,br}$* | 334 MPa (2.4%) |
| In-plane shear modulus – $G_{12}$ † | 4.9 GPa |
| In-plane shear strength – $\tau_{12}$ † | 79.1 MPa |

* Tested in accordance to ASTM D953 Procedure C [15].
† The in-plane shear properties have been derived from the UD laminate test results using classical laminate theory.

### 2.2. Experimental methodology

To fulfil the overall research aim of application in bridges, the connectors were tested under sustained (constant) as well as fully reversed cyclic loading (R = −1) as shown in Table 1. The load level applied in the long-term loading experiments was selected based on the static shear resistance experiments (series S-iSRR and S-IB) and performed in a loading rig with a jack capacity of 600kN.

The long-term loading was applied at a load level of approximately 25% of the ultimate static shear resistance. This load level was selected according to preliminary structural analyses of steel girders with FRP decks connected on top. In these analyses the load range of 40kN (equating to 25% of the ultimate shear strength) was determined as an upper bound of the alternating cyclic forces in the connectors. The same load level was selected for long-term sustained (creep) loading as it was estimated to be the upper bound of the force in the connector due to quasi-permanent load combinations.

Independent connector slip behaviour of the 2 connectors in one specimen was determined by placing a pair of linear variable differential transducers (LVDTs) on both sides of each connector. The same configuration of 4 LVDTs was used in the cyclic load experiments (series F-iSRR and F-IB), as shown in Fig. 4a. A connector displacement range increase of 0.3 mm (as investigated by [10]) was adopted as a serviceability failure criterion under long-term loading. In the cyclic loading experiments, a load ration of R = −1 was selected to investigate the loading situation where most adverse degradation rate is expected according to current literature [6]. The testing frequency was selected as 4 Hz. During the fatigue experiments, the maximum temperature increase was measured as 6 °C, which is lower than the limiting value of 10 °C as

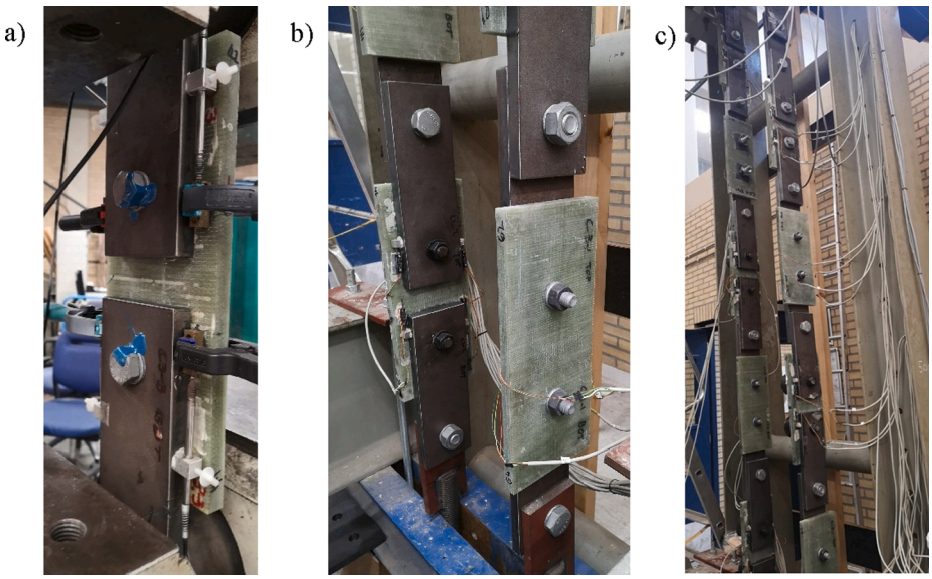


**Fig. 4.** Test set-up: (a) static and cyclic loading experiments, (b) sustained loading experiments and (c) creep tower.

stipulated in [16].

In the long-term sustained loading experiments (Series C-iSRR and C-IB), a set of 4 potentiometers per specimen (installed in a comparable manner to the aforementioned LVDTs) were used to monitor the displacement increase. In total 9 specimens = 18 connectors, including a series of blind-bolts discussed in accompanied paper [12], were connected in two long columns and hung vertically in a testing rig as shown in Fig. 4c. The desired load level was maintained by means of springs at the top of the tower and re-tensioning during the experiment.

In addition to measuring connector force–displacement behaviour by means of LVDT pairs in the S-iSRR experimental series, principle strains were also recorded by means of a GOM-ARAMIS 3D digital image correlation (DIC) system. The DIC system consists of 12 megapixel cameras calibrated to a 300 mm frame.

## 3. Results and discussion

### 3.1. Static shear resistance

The static shear resistance of the two connector types is first discussed here by analysing their load–displacement behaviour, namely initial stiffness, slip force, ultimate force and slip at failure. In addition, influence of long-term loading on short-term behaviour is compared here. Detailed results of long-term loading experiments are discussed in subsequent sub-chapters. The load–displacement curves presented in this section are selected representative curves from individual connectors. A complete set of data is given in tables.

Results of the iSRR connectors are shown in Fig. 5 (one representative connector force–displacement curve per loading regime is shown) and Table 4. Linear behaviour is observed until connector slip occurs at a force level ranging from 46.5kN to 74.3kN, corresponding to the slip resistance provided by the bolt preloading. After occurrence of subsequent slip, the connector carries an increased load until ultimate failure by crushing of the SRR injection piece, see Fig. 6, at a force level ranging from 149.7kN to 166.2kN and slip of approx. 8 mm. It is important to note that Fig. 5 displays the force–displacement curves of three representative connectors of a particular specimen, from each of the three loading regimes namely S, F and C.

The specimens subjected to long-term loading prior to static testing exhibit comparable ultimate forces and slip at failure, with up to 8% difference compared to the reference specimens subjected to static loading only. The improved performance after long-term loading is

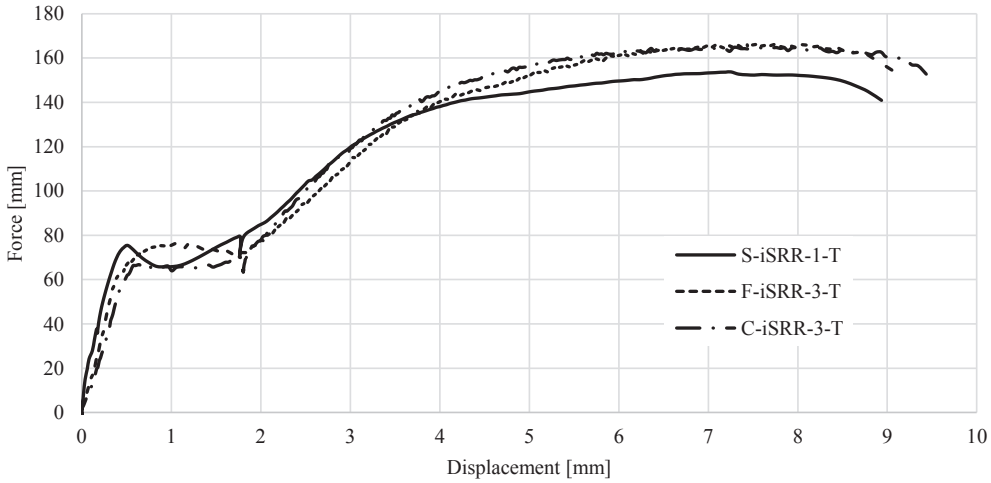


**Fig. 5.** Load-displacement curves of iSRR connectors (representative connectors selected): short-term (S-iSRR) and after sustained (C-iSRR) and/or cyclic long-term loading (F-iSRR).

**Table 4**
iSRR specimens under static loading including influence of long-term loading – average values and variations.

| | Number of specimens | Ultimate force [kN] | Initial stiffness [kN/mm] | Ultimate connector displacement [mm] | Slip force [kN] |
|---|---|---|---|---|---|
| S-iSRR | 4 | 153.9 (3.4%) | 162.0 (11.3%) | 8.5 (16.8%) | 56.4 (21.8%) |
| F-iSRR | 3 | 164.7 (0.8%) | 126.8 (27.9%) | 7.5 (25%) | 61.0 (7.3%) |
| C-iSRR | 3 | 164.7 (1.0%) | 106.0 (12.3%) | 8.5 (22.7%) | 60.9 (8.2%) |

*Coefficients of variation are stated in parentheses.

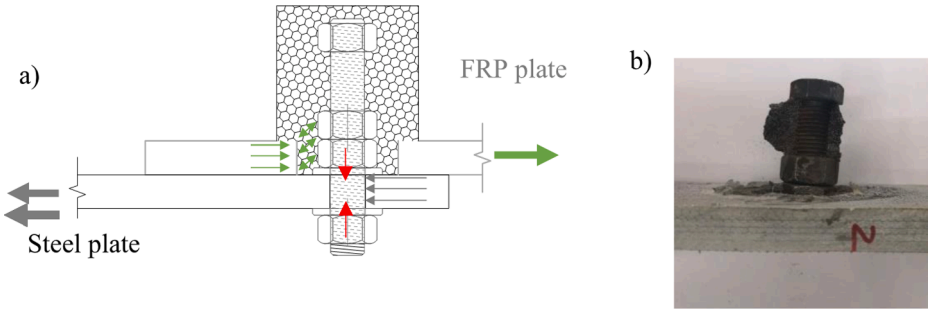


**Fig. 6.** iSRR connector behaviour: (a) load transfer mechanism; (b) failure by crushing and shattering of SRR injection piece.

attributed to additional curing effects in the iSRR. In all cases the connectors are characterised as ductile according to EN1994-1 [17], due to achieving an ultimate slip capacity of more than 6 mm.

iSRR connectors showed sufficient ductility with an ultimate displacement of more than 6.0 mm, see Fig. 5. This relatively large slip displacement at failure is attributed to use of high strength grade 10.9 steel rod which allowed mixed failure of the steel rod and SRR injection piece. This complies with the conclusions of [18] stating that an increase in ductility of bolted shear connectors embedded in concrete can be achieved by a higher strength of the mechanical connector. Specimens tested in static loading only (S-iSRR) suffered cracking starting from interface at the FRP plate. After significant deformation of the rod and subsequent cracking of the injection piece, failure of the threaded rod occurred at the shear plane coupled with sufficient energy release to break the injection piece shown in Fig. 6b. Although it is expected that such a failure mode would result in extensive scattering of the results, the failure load and displacement is quite repetitive amongst the tested specimens.

In contrast, the load transfer mechanism of the injected bolt connector relies on shearing of the bolt and bearing of the bolt in the FRP and steel plates through the thin injection medium, as shown in see Fig. 7a. In addition to shear the bolt is loaded by local bending and tensile (catenary) force as consequence of an eccentric connection. The bolt is well clamped on the side of the steel plate. The FRP plate suffers more bearing deformation leading to local bending of the bolt. Finally the governing failure mode of the IB connector subject to static loading only is by excessive bearing in the FRP plate as shown in Fig. 7b.

Results of static experiments on injected bolts are presented in Fig. 8 (showing force–displacement curves of representative connectors) and summarised with average values and coefficients of variation in Table 5. The ultimate force was on average 143 kN, 7% lower compared to iSRR. The displacement at failure is much larger, up to 10 mm, due to excessive bearing deformation in the FRP plate. In contrast to iSRR specimens, the general connector load–displacement behaviour and failure modes was not the same across all IB specimens. In Fig. 8 it is shown that ductile behaviour was obtained in all experiments with static loading only (Series S-IB). Upon the inclusion of prior long-term loading, 4 out of 7 specimens demonstrated premature bolt failure at a load level of 95 kN in average, which is 34% reduced compared to the Series S-IB. In the specimens that suffered premature bolt failure, failure of the bolt itself occurred under the head of the bolt, as indicated by the orange line in Fig. 7a. The change of failure mode is attributed to weakening of the cross-section of the bolt beneath the head during cyclic loading. At this location there is a stress concertation due to tensile (catenary) force in the bolt. To illustrate the different failure modes upon inclusion of long-term loading, in Fig. 8a distinction is made between specimens that demonstrated bolt (shown in red) or FRP bearing failure (shown in black).

To further quantify the aforementioned behaviour, Table 5 lists the initial stiffness, ultimate load and connector displacement obtained on average per experimental series.

### 3.2. Creep behaviour

Long-term experiments with sustained (creep) loading and cyclic (fatigue) loading, were performed at a tensile shear load of 40kN and load reversals of ± 40kN, respectively. In addition, to facilitate comparisons between the iSRR and IB connectors, identical loading was applied to all specimens. The same long-term loading level was applied in both the sustained and cyclic loading regimes. This (±)40kN load level was determined by means of evaluating the static resistance of both connector types in the test series S-iSRR and S-IB. This long-term load

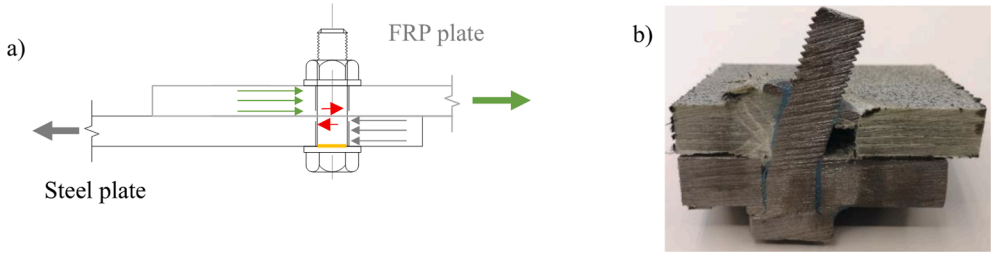


**Fig. 7.** IB connector cross-section behaviour: (a) load transfer mechanism; (b) failure in static experiment by excessive bearing.

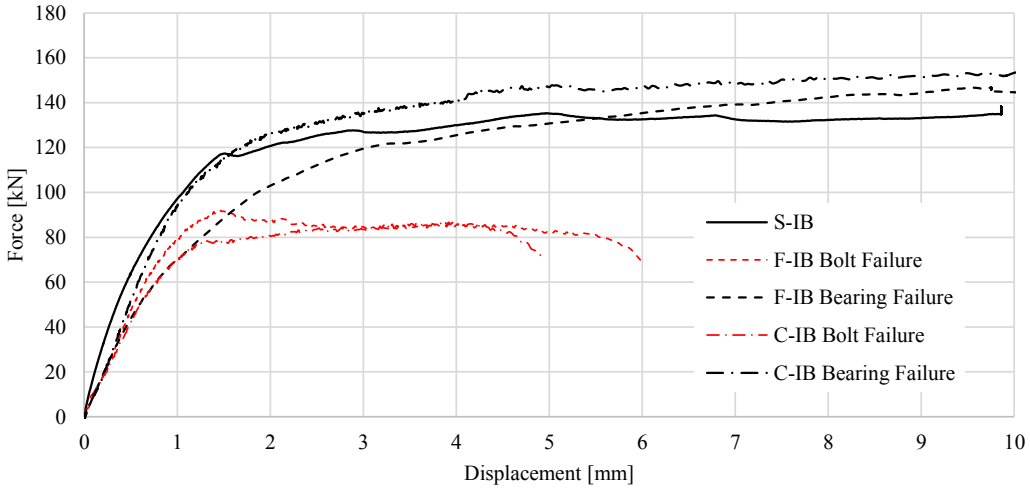


**Fig. 8.** Static resistance of (representative) IB connectors: short-term (S-IB) and after sustained (C-IB) and/or cyclic (F-IB) long-term loading.

**Table 5**
IB specimens under static loading.

| | Number of specimens | Ultimate force [kN] | Initial stiffness [kN/mm] | Ultimate connector displacement |
|---|---|---|---|---|
| S-IB | 3 | 143.5 (3.1%) | 130.0 (14.0%) | >9.5† (–) |
| F-IB | 4 | 112.5 (26.0%) | 72.1 (46.3%) | 5.8 (59.2%) |
| C-IB | 3 | 129.7 (29.0%) | 83.5 (11.6%) | 7.4 (52.6%) |

† Maximum LVDT elongation reached. *Coefficients of variation are stated in parentheses.

level equates to 25–30% of the ultimate resistance of both connector types and is assumed to be in the order of magnitude of the quasi-permanent service loads in a real bridge structure. Also, 40kN is below the experimentally measured slip force in iSRR connectors which is a requirement to foster good fatigue performance. The same holds true for the IB specimens, as no connector slip was recorded in these specimens.

The results from both connector types under sustained loading (creep) over two months, as measured on 3 specimens per connector type, each consisting of two connectors labelled top and bottom, is shown in Fig. 9a. In Fig. 9, iSRR specimens are shown in black and IB specimens in red. In this Figure, the initial displacements ($\delta_e$) resulting from the load application at the start of the experiment (40kN), as well as the displacement increase (creep displacement, $\delta_c$) under constant 40 kN loading is depicted The average values of $\delta_e$ and$\delta_c$ per connector type, as well as corresponding coefficients of variation, are listed in Table 6. The Injected bolts show in average 70% larger creep displacement ($\delta_c$) compared to iSRR connectors, as shown in Table 6, while the scattering of the creep displacement is the same for both connector types, approx. 25%.

The creep factor $\varphi(t)$ per connector was determined according to Eq. (1) and is shown in Fig. 9b. This factor is a measure of the increase in (total) displacement under sustained loading in comparison to the elastic displacement. The average creep factor per connector type, along with its corresponding coefficient of variation, is also listed in Table 6.

$$\frac{\delta}{\delta_e} = 1 + \varphi(t) => \varphi(t) = \frac{\delta}{\delta_e} - 1 \quad (1)$$

Injected bolts show a slightly lower average creep factor, 0.62 vs. 0.66 for the iSSR connectors, after 2 months of loading, albeit with double the CoV (21% vs 11%).

After two months the specimens were unloaded and monitored for 5 days to allow for recovery. On average 75% and 88% of the combined initial displacement and displacement due to sustained loading was recovered in the iSRR and IB specimens, respectively. The average residual displacement per experimental series, after the 5-day recovery period, is also listed in Table 6.

The reason for lower creep deformation of iSRR compared to the IB connectors, 0.1 mm vs 0.17 mm, see Table 6, is due to prevention of bearing deformation in the FRP plate and improved creep performance of steel-reinforced resin compared to resin alone, as found in [11]. The load transfer mechanism in the IB connector, namely bearing of a relatively small diameter bolt in FRP, results in deformation of the connector itself. This load transfer mechanism is the main contributor to the observed bolt deformation in static, but also cyclic and creep experiments of IB, see Fig. 7b. In contrast, no bearing deformation in the FRP plate was observed in the iSRR specimens, due to bearing stresses being distributed over a larger diameter (60 mm) in the FRP plate through the iSRR injection piece.

### 3.3. Fatigue behaviour

Fully reversed cycles of ±40kN shear loading in lap shear experiments was applied to at least 3 specimens (6 individual connectors) of each connector type. In addition, the specimens that were subjected to sustained (creep) loading were afterwards tested with the same cyclic loading regime.

Individual connector displacements were monitored by means of 2 pairs of LVDTs as explained in Section 2.2. The criterion to stop the cyclic loading was an increase in range of slip displacement by 0.3 mm in one of the connectors of a specimen, as discussed in Section 2.2. In case of IB it was possible to clamp the 1st connector that reached the defined criterion and continue with loading cycles for the the 2nd connector. This way, the lengthy fatigue experiments were sped up and more results are determined from a single specimen.

Fig. 10 shows the displacement increases measured per connector in case of iSRR connectors. Unfortunately, in case of iSRR connectors it was not possible to clamp the 1st failed connectors and continue testing due to the size of the SRR injection piece. This is evident in Fig. 10, where it can be seen that only one connector per specimen reached the 0.3 mm displacement criterion. It is important to note that each of the three specimens F-ISRR-1 to F-ISRR-3 consisted of 2 separate connectors (T –

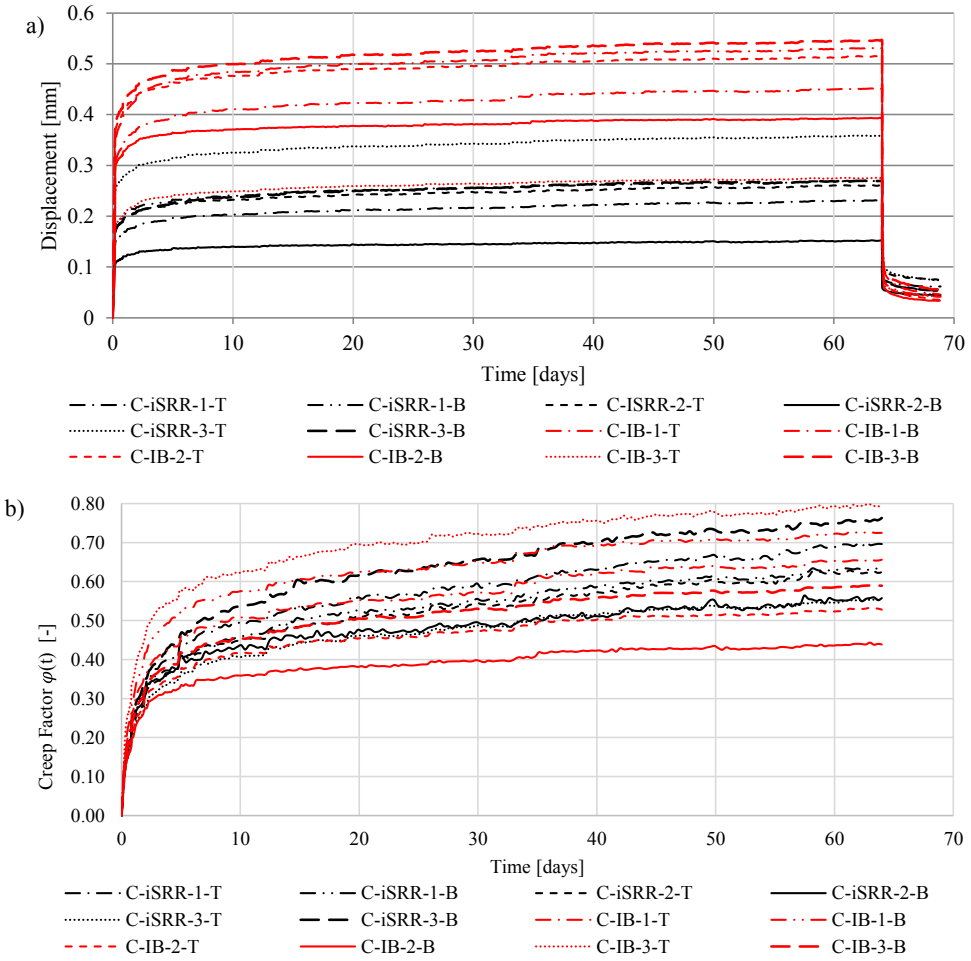


**Fig. 9.** Creep behaviour during 2 months of sustained 40kN tensile shear loading. (a) Experimental results showing elastic and creep displacement as well as the recovery phase and (b) Creep Factor.

**Table 6**
Average displacement after 2 months under sustained 40kN tensile shear loading.

| | Elastic displacement ($\delta_e$) [mm] | Creep. displacement ($\delta_c = \delta - \delta_e$) [mm] | Creep factor φ(t) [–] | Residual displacement after 5-day recovery [mm] |
|---|---|---|---|---|
| iSRR (C-iSRR) | 0.16 (27.7%) | 0.10 (25%) | 0.66 (11%) | 0.06 (18.8%) |
| IB (C-IB) | 0.28 (24.7%) | 0.17 (25%) | 0.62 (21%) | 0.04 (14.4%) |

*Coefficients of variation are stated in parentheses.

top and B – bottom). In Fig. 10a distinction is made between specimens that were tested under cyclic loading (series F – plotted in red) and specimens tested under combined sustained and cyclic loading (series C – plotted in black). The vertical axis, showing the displacement increase, is limited to the adopted displacement criterion of 0.3 mm.

Considering only the 1st connectors of each specimen, iSRR connectors reached on average 2.31 million reversed load cycles of ± 40 kN (see Table 7) when subjected to cyclic loading only (F-ISRR specimens). Specimens that were first subjected to a sustained (creep) tensile shear loading of 40 kN, reached the same criterion at 1.85 million cycles on average. To further quantify the connectors' performance, stiffness degradations are observed in Fig. 11. Stiffness of each connector is calculated by the quotient of applied force range vs. displacement range at each load cycle. The relative stiffness is then calculated at each load cycle as normalised to the stiffness obtained in the 1st load cycle. Stiffness degradation of the iSRR connectors is rather steady across the applied load cycles, reaching on average 45% upon reaching the 0.3 mm assumed criterion. Specimens that were prior subjected to sustained loading (C-ISRR specimens) have comparable (44%) stiffness degradation on average.

The increase of slip displacement against the number of cycles in case of injected bolt connectors is shown in Fig. 12. In this case it was possible to continue testing the 2nd connector of a specimen after the 1st specimen reached the 0.3 mm additional slip displacement. On average IB connectors (specimens F-IB) reached 23.7 thousand cycles until reaching the 0.3 mm criterion, see Table 7. Scattering of the results is huge. On average, when sustained (creep) loading is applied prior to cyclic loading, unexpectedly a higher number of cycles, 27.9 thousand (specimens C-IB), is achieved.

Less degradation of relative stiffness in individual IB connectors compared to iSRR connectors was recorded, approximately 30% at reaching the 0.3 mm criterion, as shown in Fig. 13. This is attributed to larger initial displacements of those connectors having smaller diameter than the iSRR connectors.

As an overall summary of the various cyclic loading experiments, Table 7 lists the average number of loading cycles and coefficients of variation (CoV) as measured per connector and loading type (without and with prior sustained loading).

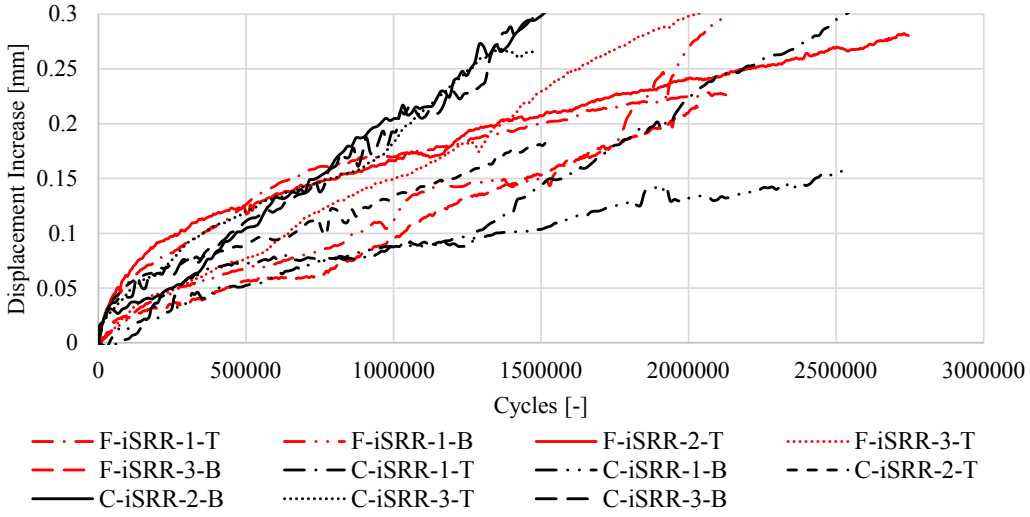


**Fig. 10.** Increase of iSRR connector displacement (slip) due to ±40 kN cyclic loading, equivalent to ±25% of shear resistance.

**Table 7**
Sustained reversed loading cycles of ± 40 kN of iSRR and IB connectors until reaching 0.3 mm additional slip displacement.

| | F-iSRR | C-iSRR | F-IB | C-IB |
|---|---|---|---|---|
| Average [cycles] | 2.31E+06 | 1.85E+06 | 23.73E+03 | 27.87E+03 |
| CoV [%] | 16.5 | 32.1 | 65.3 | 48.8 |

None of the connectors reached the final failure at the indicated number of cycles. This is attributed to the selected 0.3 mm displacement increase criterion, which was used to facilitate fatigue performance comparisons of the two connector types. However, all specimens were tested in a static loading regime to determine the residual static resistance, which is presented in Section 3.1.

As presented by the results, the iSRR connectors behave much better compared to IB connectors in cyclic, creep and residual static experiments. This is related to the load transferring mechanism that relies on preloading of the bolt and large bearing area (⌀60 mm, t = 20 mm) in the FRP plate, see Fig. 6a. The preloading is applied within the clamping package that only encompasses steel components; therefore no loss of the preloading force is experienced. This hypothesis is confirmed by the same level of slip resistance of S-iSRR series (static only) and C-iSRR series (creep + cyclic + static) in Fig. 5.

The much better fatigue performance, 2 million vs. 20 thousand cycles, of the iSRR compared to IB connectors is attributed to the load transferring mechanism relying on preloading of the bolt which prevents shear stress cycles in the bolt. The number of cycles for IB connectors is considerably scattered and inconclusively low at the considered load level of ±40 kN shear load. This relatively high load level was chosen in order to allow comparison and quantify the potential of the novel iSRR vs. concurrent slip-resistant connectors, such as injected bolts. The hypothesis is that a much larger diameter of injected bolts can be used to reach the same fatigue performance of iSRR connectors. Further fatigue tests at different load levels are needed to fully characterise fatigue performance and provide S-N curves for iSRR connectors.

Prior creep testing had an influence on the fatigue performance of the iSRR connectors. The number of cycles to reach the 0.3 mm displacement criterion was reduced by 20% and the CoV approximately doubles. The hypothesis is that larger scatter of fatigue results in specimens with prior creep loading is owing to two phenomena: 1) generation of initial gap in injection or FRP material due to creep and 2) additional 4 months of post-curing due to creep tests. The former is supposed to worsen the fatigue performance, approx. 16% of degradation of initial stiffness in reversed load cycles was experienced. The latter is expected to improve it, therefore widening the pool of specimen

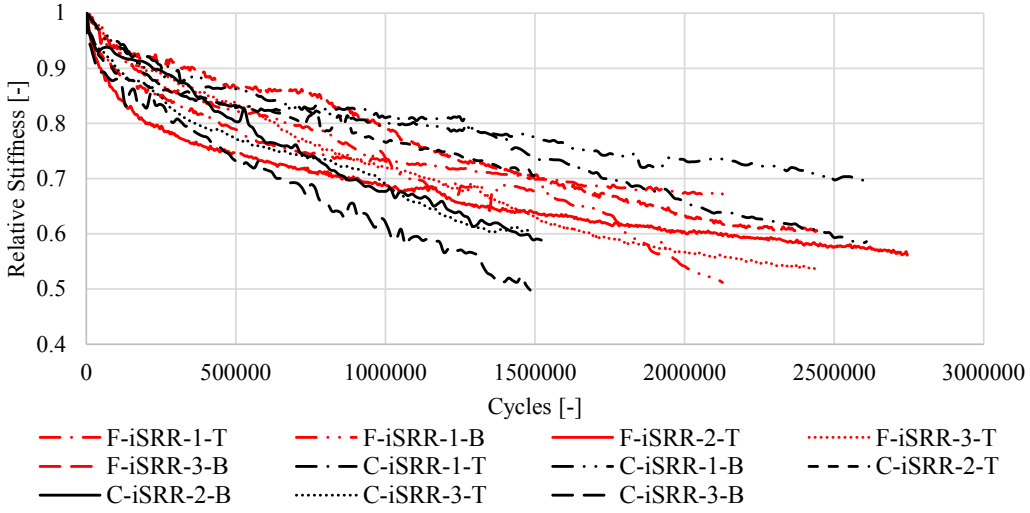


**Fig. 11.** Relative Stiffness decrease of iSRR connectors under cyclic loading.

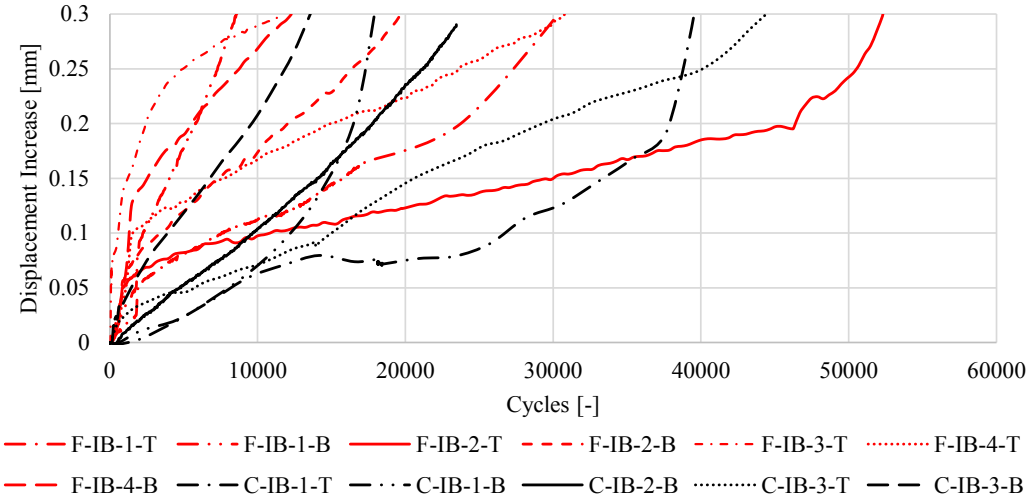


**Fig. 12.** Displacement increase of IB connectors due to cyclic loading.

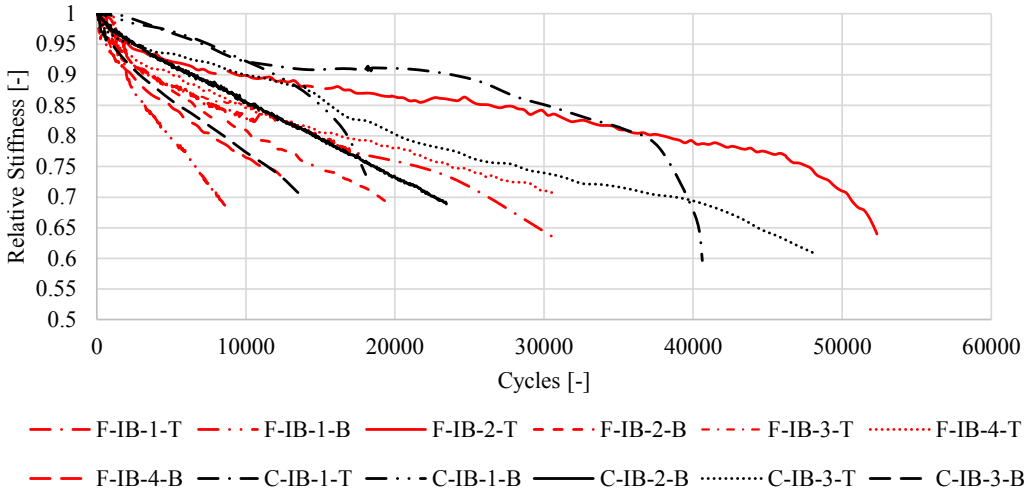


**Fig. 13.** Relative stiffness decrease of IB connectors under cyclic loading.

variable performances. In real bridge applications it is hardly expected that such "worst case scenario" exists, combining large sustained connector shear force in one direction (creep) and fully reversed load cycle due to fatigue loading of traffic and temperature. The influence of creep on the fatigue performance of IB connectors is inconclusive due to the large scattering of the results.

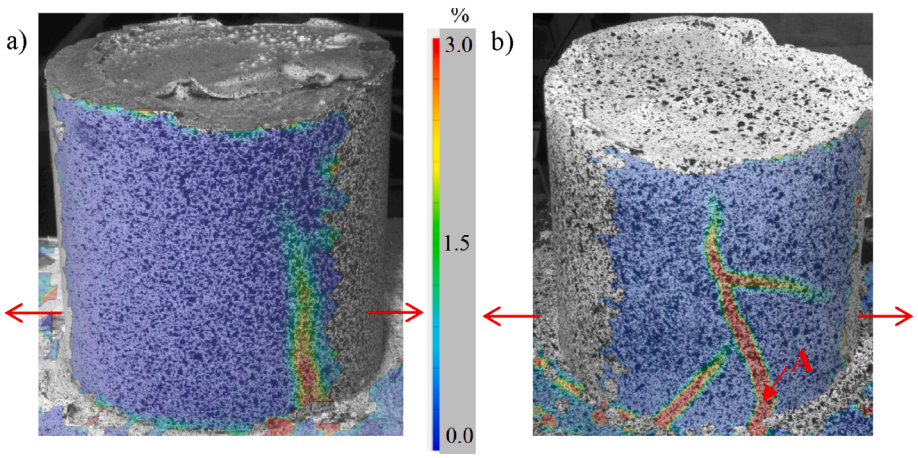


**Fig. 14.** iSRR connector major principal strain at 100kN loading (loading direction marked with red arrows): (a) specimen with static loading only, (b) specimen with static loading after long-term loading. (For interpretation of the references to colour in this figure legend, the reader is referred to the web version of this article.)

No reduction of static resistance is found for the iSRR connectors after approx. 2 million of load cycles, whilst approx. 60% of IB specimens experienced reduction of static resistance up to 34% after only 30 thousand cycles, see Fig. 8.

### 3.4. Damage tolerance of iSRR connectors

The observed failure mode in the static experiment is bolt failure followed by severe crushing/cracking of the SRR injection piece. Development of crack at location A on the surface of the iSRR injection piece, see Fig. 14b, was also observed during the fatigue experiment. The crack initiates and develops to a stable length relatively early, within the first few thousand cycles. However, this initial crack does not lead to considerable fatigue damage, apparent by e.g. a drop in stiffness during the remaining cyclic loading, see Fig. 11. The question was if this cracking behaviour will severely influence the residual static resistance of iSRR connectors. In order to track the development of the crack on the surface of the iSRR injection piece, measurements of principle strains were taken by means of 3D DIC system.

Fig. 14 depicts the cracks identified using major principal strains obtained by a 3D DIC system. The limit on strain visualisation is set to 3% to indicate crack paths in zones where the cracking limit in order of magnitude of greater than 1–2% can be expected for a polymeric composite material, such as the iSRR injection piece. Two representative connectors from series of specimens being tested by static load only and static after creep and fatigue loading, S-ISRR and C-ISRR respectively, are shown at a load level of 100kN. The crack in the specimen which was loaded by prior cyclic loading is fully developed at this load level but the slip displacement is only 10% larger compared to the specimen without prior fatigue loading, see Fig. 5. Plotted in Fig. 15 are crack opening widths with increase static test load, measured along the length of the crack starting with the origin at point A (at the interface of the injection piece and FRP plate) and propagating in the direction of the top of the iSRR connector.

Fig. 15a shows that the crack opens in specimen loaded by static load only at a load level of 74kN and as soon as at a load level of 6 kN in the specimen previously subjected to cyclic loading, Fig. 15b. The maximum crack length in the latter case stabilises at approximately 50kN. The conclusion is that the crack on the surface of the iSRR injection piece developed by loading cycles does not compromise the static resistance of the connector. A potential risk, however, is water ingress due to presence of the crack, leading to corrosion of the steel spheres and the steel bolt, as well as freeze thaw action. It is expected that this would not be an issue for the application of iSRR connectors in FRP decks, where the connector is enclosed inside the FRP deck panel, see Fig. 1b.

## 4. Conclusions

This study compares the short- and long-term behaviour of 2 types of slip-resistant connectors for hybrid steel-FRP structures: novel iSRR-connectors and injected bolts. Shear experiments in a single lap joint configuration are used to characterise static, fatigue and creep behaviour. A serviceability criterion of an increase in slip displacement of 0.3 mm was used to compare the fatigue performance. The novel iSRR connector demonstrates great potential as a slip-resistant connector in hybrid steel-FRP structures based on the following findings:

1. The initial stiffness in the order of magnitude of 100 kN/mm, shear resistance of up to 160 kN and ultimate slip at failure of above 8 mm are comparable for both connector types.
2. The iSRR connectors sustained on average 2.31 million fully reversed shear load cycles of ± 40 kN before slip was increased by 0.3 mm. The degradation curves of 5 connectors are steady and consistent, leading to a coefficient of variation of the number of cycles CoV = 16%. The fatigue endurance of injected bolts was on average 100 times less: 23.7 thousand load cycles at the same load regime, accompanied by a large scattering (CoV = 65%). Connector fracture was not observed during any of the fatigue experiments. Advantageous fatigue performance of iSRR is attributed to load transferring mechanism relying on preload and friction.
3. Application of load cycles resulted in a change of static failure mode from quasi-ductile FRP bearing failure to a brittle bolt failure in conventional injected bolt connectors. Brittle bolt failure was found in 60% of the conventional injected bolt specimens subjected to static loading after cyclic loading. The result of brittle failure is 34% reduction of residual static resistance. In contrast, the residual resistance of the iSRR connectors after long-term loading is equal to the short-term static shear resistance.
4. The iSRR connectors demonstrated 0.1 mm additional creep deformation after 2 months of sustained loading. Conventional injected bolts yielded a 72% higher additional creep deformation.
5. A slip displacement increase criterion of 0.3 mm was reached 20% sooner in iSRR specimens previously subjected to sustained (creep) loading. The effect of creep on fatigue performance of IB is inconclusive due to large scattering.

### CRediT authorship contribution statement

**Gerhard Olivier:** Methodology, Validation, Data curation, Writing – original draft, Visualization. **Fruzsina Csillag:** Methodology, Validation, Writing – review & editing. **Elisabeth Tromp:** Conceptualization,

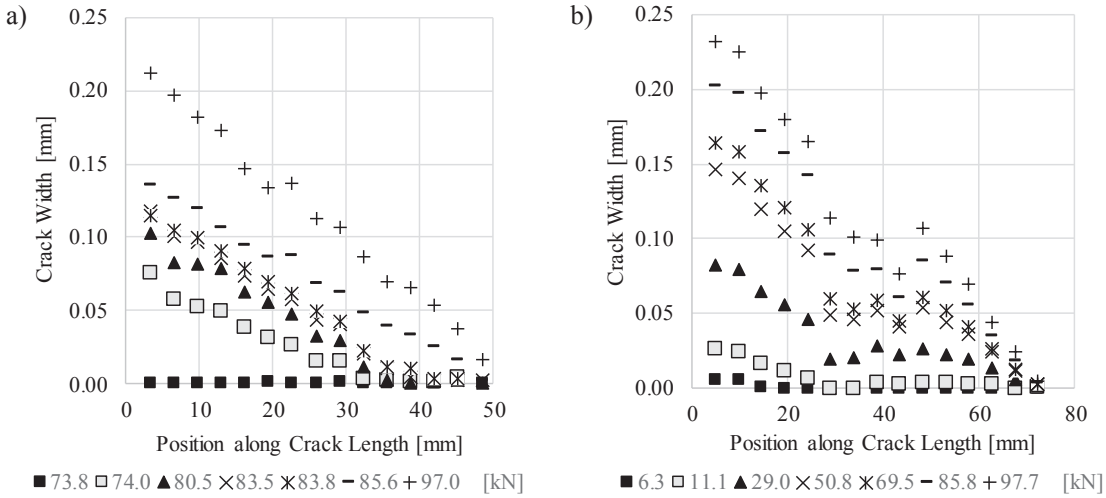


**Fig. 15.** Crack opening at different load level along crack: (a) specimen with static loading only, (b) specimen with static loading after long-term loading.

Supervision. **Marko Pavlović:** Supervision, Methodology, Writing – review & editing, Project administration, Funding acquisition.

## Declaration of Competing Interest

The authors declare that they have no known competing financial interests or personal relationships that could have appeared to influence the work reported in this paper.

## Acknowledgements

The authors are very grateful to Rijkswaterstaat, the Dutch Ministry of Infrastructure, for supporting the research. Furthermore, thanks are due to Aliancys b.v. for supplying the resin used in the iSRR connectors and FiberCore Europe b.v. for producing the specimens.

## References

[1] Keller T, Gürtler H. Design of hybrid bridge girders with adhesively bonded and compositely acting FRP deck. Compos Struct 2006;74(2):202–12. https://doi.org/10.1016/j.compstruct.2005.04.028.
[2] Moon FL, Eckel DA, Gillespie JW. Shear stud connections for the development of composite action between steel girders and fiber-reinforced polymer bridge decks. J Struct Eng 2002;128(6):762–70. https://doi.org/10.1061/(ASCE)0733-9445(2002)128:6(762).
[3] Nijssen R, van Wingerde A, van Delft D. The OptiDAT materials fatigue database. In: Lilholt H, Madsen B, Andersen T, Mikkelsen L, Thygesen A, editors. 27th Riso Int. Symp. Mater. Sci. Polym. Compos. Mater. Wind power turbines, Roskilde, Denemakrken: Riso National Laboratory; 2006, p. 257–63.
[4] Vassilopoulos AP, Keller T. Fatigue of fiber-reinforced composites. Springer Science & Business Media; 2011.
[5] Wu C, Feng P, Bai Y. Comparative study on static and fatigue performances of pultruded GFRP joints using ordinary and blind bolts. J Compos Constr 2015;19. https://doi.org/10.1061/(ASCE)CC.1943-5614.0000527.
[6] van Wingerde AM, van Delft DRV, Knudsen ES. Fatigue behaviour of bolted connections in pultruded FRP profiles. Plast, Rubber Compos 2003;32(2):71–6. https://doi.org/10.1179/146580103225009103.
[7] Smith PA, Pascoe KJ. Fatigue of bolted joints in (0/90) CFRP laminates. Compos Sci Technol 1987;29(1):45–69. https://doi.org/10.1016/0266-3538(87)90036-4.
[8] ASTM D953 – 02. Standard test method for bearing strength of plastics. Annu B ASTM Stand; 2002.
[9] Zafari B, Qureshi J, Mottram JT, Rusev R. Static and fatigue performance of resin injected bolts for a slip and fatigue resistant connection in FRP bridge engineering. Structures 2016;7:71–84. https://doi.org/10.1016/j.istruc.2016.05.004.
[10] EN 1090-2. Execution of steel structures and aluminium structures – Part 2: Technical requirements for the execution of steel structures. Brussels, Belgium; 2008.
[11] Nijgh MP. New materials for injected bolted connections a feasibility study for demountable connections. Delft University of Technology; 2017.
[12] Olivier G, Csillag F, Tromp E, Pavlović M. Static, fatigue and creep performance of blind-bolted connectors in shear experiments on steel-FRP joints. Eng Struct 2021;230:111713. https://doi.org/10.1016/j.engstruct.2020.111713.
[13] Csillag F, Pavlović M. Push-out behaviour of demountable injected vs. blind-bolted connectors in FRP decks. Submitt Compos Struct 2020.
[14] CROW. CUR 96: Fibre reinforced polymers in civil load bearing structures; 2019.
[15] ASTM D953 – 18. Standard test method for pin-bearing strength of plastics. Annu B ASTM Stand; 2018. https://doi.org/10.1520/D0953-10.2.
[16] International Organization for Standardization. NEN-ISO 13003: Fibre-reinforced plastics—determination of fatigue properties under cyclic loading conditions; 2003.
[17] EN1994-1-1. Eurocode 4: Design of composite steel and concrete structures – Part 1-1: General rules and rules for buildings. Brussels, Belgium; 2005.
[18] Pavlović M. Resistance of bolted shear connectors in prefabricated steel-concrete composite decks. Belgrade: University of Belgrade; 2013.